

AD C 027914

ROSENSTIEL SCHOOL OF MARINE AND ATMOSPHERIC SCIENCE

UNIVERSITY OF MIAMI

4600 RICKENBACKER CAUSEWAY

MIAMI, FLORIDA 33149

THE M7 COMMUNICATION SYSTEM

FINAL REPORT OF CONTRACT

NO. N00014-80C-0418

CLASSIFIED BY: NAVINST C5511.5 OF 1 OCT 74

~~EXEMPT FROM GDS OF EO 11652~~

~~EXEMPTION CATEGORY: 3~~

DECLASSIFY ON: 31 DECEMBER 2007

DECLASSIFIED BY: Chief of Naval Research  
DATE: 7 April 2021

CHRISTOPHER V. KIMBALL

26 JULY 1979

DTIC FILE COPY

COPY NUMBER: 3 OF 44

DTIC  
ELECTE  
S APR 20 1982 D  
A

82 9 12 521



[REDACTED]

ROSENSTIEL SCHOOL OF MARINE AND ATMOSPHERIC SCIENCE

UNIVERSITY OF MIAMI  
4600 RICKENBACKER CAUSEWAY  
MIAMI, FLORIDA 33149

THE M7 COMMUNICATION SYSTEM [REDACTED]

FINAL REPORT OF CONTRACT

NO. N00014-80C-0418

CHRISTOPHER V. KIMBALL

26 JULY 1979

[REDACTED]



SECURITY CLASSIFICATION OF THIS PAGE (When Data Entered)

REPORT DOCUMENTATION PAGE		READ INSTRUCTIONS BEFORE COMPLETING FORM	
1. REPORT NUMBER	2. GOVT ACCESSION NO. <b>AD-C027914</b>	3. RECIPIENT'S CATALOG NUMBER	
4. TITLE (and Subtitle) <b>THE M7 COMMUNICATION SYSTEM FINAL REPORT OF CONTRACT NO. N00014-80-C-0418</b>		5. TYPE OF REPORT & PERIOD COVERED <b>FINAL REPORT</b>	
7. AUTHOR(s) <b>Christopher V. KIMBALL</b>		6. PERFORMING ORG. REPORT NUMBER	
9. PERFORMING ORGANIZATION NAME AND ADDRESS <b>Rosenstiel School of Marine and Atmospheric Science University of Miami, 4600 Rickenbacker Causeway Miami, Florida 33149</b>		8. CONTRACT OR GRANT NUMBER(s) <b>N00014-80C-0418</b>	
11. CONTROLLING OFFICE NAME AND ADDRESS <b>ONR Research Representative, Georgia Institute of Technology, Room 325, Finman Research Building Atlanta, Georgia 30332</b>		10. PROGRAM ELEMENT, PROJECT, TASK AREA & WORK UNIT NUMBERS <b>531221</b>	
14. MONITORING AGENCY NAME & ADDRESS (if different from Controlling Office) <b>Director Sensor and Control Technology Division, Technology Programs, Office of Naval Research, 800 N. Quincy Street. Arlington, Virginia 22217</b>		12. REPORT DATE <b>26 July 1979</b>	
		13. NUMBER OF PAGES <b>183</b>	
		15. SECURITY CLASS. (of this report) <b>[REDACTED]</b>	
15. DISTRIBUTION STATEMENT (of this Report) <b>"Distribution shall be only as prescribed by the Scientific Officer."</b>		16. DECLASSIFICATION/DOWNGRADING SCHEDULE <b>NAVINST C5511.6;DECL:31Dec2007</b>	
17. DISTRIBUTION STATEMENT (of the abstract entered in Block 20, if different from Report)			
18. SUPPLEMENTARY NOTES			
19. KEY WORDS (Continue on reverse side if necessary and identify by block number) <b>Acoustic Communication Studies Summary Acoustic Fluctuations</b>			
20. ABSTRACT (Continue on reverse side if necessary and identify by block number) <b>The M7 underwater acoustic communication system developed by the Acoustic Communication Studies Project of the University of Miami as described. This system is designed to reduce the transmitted energy per received bit and to reduce the vulnerability of the transmitting platform to detection by hostile receivers. Three techniques are used to accomplish these objectives: a freely randomisable pseudo-noise transmission format, true matched filter reception, and coherent integration.</b>			

DD FORM 1 JAN 73 1473

EDI

DELETE

SECURITY CLASSIFICATION OF THIS PAGE (When Data Entered)



## ITEM 20 CONTINUED

Five independently written papers follow a brief introduction in this report. These papers provide an overview of system objectives and techniques, followed by more detailed explanation of actual receiver operation. Finally, a discussion of the relevance of the Mobile Acoustic Communication Study (MACS) results available to date is included.



# ABSTRACT

■ The M7 underwater acoustic communication system developed by the Acoustic Communication Studies Project of the University of Miami as described. This system is designed to reduce the transmitted energy per received bit and to reduce the vulnerability of the transmitting platform to detection by hostile receivers. Three techniques are used to accomplish these objectives: a freely randomizable pseudo-noise transmission format, true matched filter reception, and coherent integration.

■ Five independently written papers follow a brief introduction in this report. These papers provide an overview of system objectives and techniques, followed by more detailed explanation of actual receiver operation. Finally a discussion of the relevance of the Mobile Acoustic Communication Study (MACS) results available to date is included.



Accession For	
NTIS GRA&I	<input type="checkbox"/>
DTIC TAB	<input checked="" type="checkbox"/>
Unannounced	<input type="checkbox"/>
Justification	
By _____	
Distribution/ _____	
Availability Codes	
Dist	Avail and/or Special
9	



## FORWARD

■ The University of Miami Acoustic Communication Studies project has been terminated without the sea evaluation recommended by both ONR and NOSC. Consequently, this final report is presented without any at sea performance data. Earlier experimental results and recent simulation data suggest the system would provide significant ( $\sim 10\text{dB}$ ) performance advantages relative to a comparable incoherent tonal system, but a side-by-side evaluation of the two systems proposed for the summer of 1979 was denied. The Navy's failure to evaluate the M7 system either independently or in comparison with the tonal system has been a disappointment to the author.

■ Five papers have been bound together for this report. The first gives a brief overview of the system goals, techniques and capabilities. The second provides a detailed description of the signal format and receiver operation. In the third paper, the results of an extensive simulation of receiver operation under realistic operating conditions is presented. In the fourth paper, the hardware requirements for implementation of the system are described. Finally, the fifth paper comments on the coherence time results obtained by the Mobile Acoustic Communication Studies (MACS) project and their relevance to large time bandwidth product systems such as M7.



#### ACKNOWLEDGEMENTS

■ The determined support of Dr. A. O. Sykes of the Office of Naval Research (Code 222) and Mr. Darrell E. Marsh of the Naval Ocean Systems Center (Code 7123) is gratefully acknowledged. Important contributions to the project were made by Dr. Chester A. Jacewitz.



TABLE OF CONTENTS ■

ABSTRACT

FOREWORD

ACKNOWLEDGEMENTS

- PART 1: THE M7 COMMUNICATION SYSTEM: AN OVERVIEW ■
- PART 2: A GUIDE TO THE PARAMETERS AND OUTPUT OF THE M7 COMMUNICATION SYSTEM ■
- PART 3: PERFORMANCE OF THE M7 SYSTEM SIMULATION ■
- PART 4: COMPUTER REQUIREMENTS FOR THE M7 COMMUNICATION SYSTEM
- PART 5: COMMENTS ON THE MACS COHERENCE TIME MEASUREMENTS ■

DISTRIBUTION LIST

DD FORM 1473

■

## LIST OF FIGURES

<u>Figure</u>	<u>Title</u>	<u>Page</u>
1	M7B Computer Programs	3
2	M7BX2 Transmission Example	8
3	Digit Modulation Alternatives	10
4	Block Summary: Identifying Labels	14
5	Receiver Operation Overview	16
6	Search Procedure	20
7	Block Summary: Synchronization Outputs	24
8	Demodulation Flow Chart	26
9	Block Summary: Initial Demodulation Outputs	32
10	Block Summary: Bootstrap Demodulation	35
11	Page and Line Summaries	38
12	Teleprinter Output	41



PART 1

THE M7 COMMUNICATION SYSTEM:  
AN OVERVIEW

26 JULY 1979



[REDACTED]

The M7 Communication System: An Overview [REDACTED]

[REDACTED] The M7 communication system is the seventh experimental underwater acoustic communication system developed at the Universities of Miami and Michigan during the interval 1967-1979. It is distinctly different from the incoherent, tonal signalling systems currently in use or proposed. The two major considerations in its design were the minimization of transmitted energy per information bit and the reduction of the vulnerability of the transmitting platform to hostile detection. With appropriate choice of parameters the system can be configured for either tactical or strategic applications, the example presented below is on the borderline between these two applications. The M7 system has been ready for evaluation at sea since June 1978, an opportunity perform the evaluation is still being sought.

[REDACTED] The fundamental technique of the M7 system is based on classical signal detection theory for a signal known exactly in added white Gaussian noise. Under such conditions, the optimum (likelihood) receiver is a filter matched to the received signal followed by a threshold detector. Since a practical acoustic channel does not yield a response known a priori, the M7 system performs a measurement of the channel impulse response prior to the information processing. Although the details of the signal processing and parameter values are different, the operation of the system is analogous to the "RAKE" HF modem described by Price and Green in 1958.

[REDACTED] In order for the above technique to be applicable, the acoustic channel must be linear and time-invariant over the channel measurement time. For fixed site channels and center frequencies below 500 Hz, this result has been established for measurement times of the order of minutes. Experiment with towed sources conducted off Eleuthera (400 Hz, 1974) Bermuda (313 Hz, 1976) indicated measurement times of the order of a minute would be satis-

[REDACTED]



[REDACTED]

factory. As the system center frequency is decreased, these times can be expected to increase further.

■ To reduce the detectability of the transmitted signal by hostile receivers, a pseudo-noise transmission format was selected. This makes detection by narrow band spectral analysis futile, particularly when the received signal level is low (below 0 dB), which is the system's intended operating condition. For the hostile detector the problem becomes one of detecting noise-like signals in the fluctuating ambient noise of the ocean.

■ The pseudo-noise transmission format is also an excellent one for purely communication purposes, as the signal is uniformly distributed over the available bandwidth. Equivalently, the pseudo-noise format can be considered to offer a very large degree of frequency diversity.

■ Three basic features are incorporated into the M7 system: freely randomizable choice of pseudo-noise wave form, true matched filter processing, and coherent integration. Other included features such as the synchronization/Doppler removal algorithms and the provision for m-ary biorthogonal signalling are beyond the scope of this paper.

■ The transmitted waveform in the M7 system is based on a binary sequence known to both the transmitter and intended receiver. This sequence must have the statistical properties (particularly bias and auto correlation properties) of a random bit stream and could be conveniently be provided by an approved cryptologic generator and changed on a code-of-the-day basis. The sequence need not obey any deterministic mathematical law, such as the linear maximal sequences commonly employed in scientific channel measurement programs. Further, the randomness of the transmission is unaffected by the particular message being sent. With

[REDACTED]

[REDACTED]

this freely randomizable design, the system satisfies the "cryptologic postulate" in that an interceptor equipped with the same receiving equipment as the intended receiver has no detection advantage unless he knows the prescribed bit stream.

■ The second feature of the M7 system is its measurement of the channel impulse response with each transmission. This measurement is possible because the transmission includes a known component, called the probe, which also is used for time and frequency synchronization. The channel impulse response is extracted from the received signal through a correlation and filtering algorithm. Then filters for each of the information-bearing symbols are constructed through the assumed linearity of the channel and the knowledge of the symbol alphabet. Because both probe and information components pass through the channel at the same time, the exact instant for sampling the symbol filter outputs is known and no "soft decoding" algorithm need be applied.

■ The sharp contrast in approaches to channel variations between the M7 system and conventional incoherent tonal systems must be noted. A typical tonal system represents a compromise in design parameters to allow operation at different ranges and locations. Extensive statistical studies of channel responses have been made to facilitate this compromise. The M7 system, through its on-the-spot channel measurement, designs its receiving filters for exactly the channel at hand.

■ Finally, the M7 system uses coherent integration for synchronization, channel measurement and information processing. This allows useful operation at signal to noise ratios well below 0 dB.

[REDACTED]



[REDACTED]

■ To provide a tangible example of the M7 system, consider the most recent version, M7BX3. The transmission for this version occupies a 51.2 Hz (at 4 dB points) bandwidth centered on 204.8 Hz, so that each burst has a time-bandwidth product of 4096. Sixty information bits are contained in each burst, yielding a bit rate of .75 bits/sec. Simulation results based on a measured 350 nm channel and worst case (21.5 kt) Doppler conditions show the system does not miss any bursts (out of 512) at -10 dB signal to noise ratio. The probability of a symbol error at this signal to noise ratio is .0078, which is equivalent to a bit probability of error of .0016. At an input signal to noise ratio of -7 dB, the probability of a symbol error falls to .000173, which is equivalent to a bit probability of error of .000029. Note that these error probabilities are obtained at the receiver filter output and have not been enhanced through error correcting codes. When compared with theoretical values for a competitive incoherent tonal system, these results indicate a 10 dB advantage for the M7 system.

■ The issue of hardware implementation of the M7 system is an important one because the M7 does place different requirements on the hardware, specifically in terms of calculational speed and memory size. Nevertheless satisfactory hardware is currently available based on a military-qualified version of the PDP-11 computer and an array processor built to be in compliance with military standards. This hardware occupies 3.52 cubic feet (4 ATR modules) including space for interface electronics. The cost per unit (based on a 4 unit purchase) is \$313,000 with delivery within 6 months. These costs do not include that for the interface circuitry which is application dependent. With this hardware the M7BX3

[REDACTED]

[REDACTED]

version could be operated with at least a  $\pm$  kt Doppler uncertainty in a single channel mode or a low-Doppler strategic System could be operated on eight channels.

#### References [REDACTED]

1. R. Price and P. E. Green, "A Communication Technique for Multi-path Channels," Proceedings of the IRE, March 1958.
  2. C. V. Kimball, "Acoustic Communication Studies [REDACTED]," Journal of Defense Research, Series B: Tactical Warfare, Summer 1975 [REDACTED].
  3. C. V. Kimball, letter to Dr. A. O. Sykes, Office of Naval Research (Code 222), dated 19 February 1979 [REDACTED].
  4. C. V. Kimball, letter to Dr. Daniel M. Viccione, Naval Underwater Systems Center, New London Laboratory (Code TC), dated 13 March 1979 [REDACTED].
- [REDACTED]



PART 2

A GUIDE TO THE PARAMETERS AND  
OUTPUT OF THE M7 COMMUNICATION SYSTEM ■

ORIGINAL VERSION: 6 JUNE 1978

REVISED: 6 June 1979

## CONTENTS ■

	Page
1. Introduction	1
2. General System Operation	2
3. Transmission Format	4
4. Receiver Operation and Results	12
4.1 General Operation	12
4.2 Synchronization	17
4.3 Demodulation	25
4.3.1 Initial Demodulation	25
4.3.2 Bootstrap Demodulation	33
4.4 Other Receiver Outputs	37
4.4.1 General	37
4.4.2 Line Summaries	37
4.4.3 Page Summaries	39
4.4.4 Teleprinter Output	40
4.4.5 Oscilloscope Display	40
4.4.6 Magnetic Tape	42



[REDACTED]

Preface to the Revision of 6 June 1979

Three minor changes were made in the year since the original report was written.

First, a limit, ZSHLIM, on the magnitude of the fine-grain frequency shift performed by ZSHIFT was incorporated. This prevents the ZSHIFT algorithm from radically modifying the signal frequency when the signal to noise ratio is too low for a correct fine-grain frequency measurement.

Second, the search algorithm has been applied after the ZSHIFT in the initial demodulation. This post-ZSHIFT search improves the frequency synchronization on the initial demodulation and leads to better initial symbol decisions.

Third, the nomenclature for the statistical output variables has been improved. Appendix A gives translation tables between versions. The new nomenclature for an output variable XXN tells which stage N the variable XX was computed:

<u>N</u>	<u>Stage</u>
0	Primary Search
1	Secondary Search
2	Initial Demodulation
3	Bootstrap Demodulation

This change does not apply to input variables, i.e., R2CUT $\phi$  is used on all applications of the ZSHIFT algorithms, not to the primary search.

[REDACTED]

## 1. Introduction

The objective of this paper is to provide a guide for the interpretation of results from the M7 receiver, so that its capabilities can be understood prior to an experiment at sea. Although no attempt is made to explain the theoretical and engineering considerations behind the M7 system, sufficient background to understand the various parameters is provided. After a quick overview of system operation, a detailed description of the transmission format is given. This is followed by a description of the outputs corresponding to both synchronization and information processing stages of the receiver.

## 2. General System Operation

The operation of the M7 communication system is based on a random bit stream known only to the transmitter and receiver. Such a bit stream, along with identifying labels, is referred to as a KFILE, where the "K" is for "key stream". Specific KFILES are generated by undersampling a laboratory thermal noise source. Since no communication is possible if the transmitter and receiver are using different KFILES, great care is taken to avoid mixed usage!

The M7 transmitter generates the M7 communication signal, as well as a number of classical channel measurement signals such as CW, coherent pulses and periodic pseudo-random sequences. In the M7 mode, the KFILE and receiver parameters are entered by the operator. Errors in the KFILE or between the KFILE parameters and those specified by the operator are automatically indicated. The operator also enters the message in either hexadecimal or radix 40 (A-Z, 0-9, ?/\*-) notation and starts the transmission. Transmissions can be sent either one at a time or periodically at a specified



delay. Provision for a continuous carrier (CW) while in this mode is available, with the carrier to burst energy ratio adjustable from 1 to 0 (during the burst).

■ The M7 receiver is a flexible system for detecting and processing the transmission, the details of which are beyond the scope of this note. Because a particular version of the M7 system requires the specification of 27 parameters, a set of parameters and an identifying label for a particular version of the system are placed in a file, called the RFILE (R for "receiver") for use when required. Operation of the receiver requires the presence of precomputed vectors on another file. These vectors are calculated from the parameters and the specific KFILE in use; the file that contains them is called the VFILE (V for "vector"). When the receiver is started, the correspondence between the parameters of the RFILE and the VFILE is verified. The interrelation of the various files and the programs that generate them is shown in Figure 1.

■ Many outputs are available during the operation of the receiver. If the input is from an analog source, an industry-compatible (IBM) tape can be written, containing all the unprocessed input samples. Approximately 24 hours can be placed on one tape, which can then be reprocessed by the receiver with different parameters (i.e. a different RFILE). A conventional teleprinter allows operator control and provides a single line containing the time and information content (in both hexadecimal and radix 40 notation) for each burst received. A line printer provides more detailed information in several forms. First, a single line is typed for each burst, giving 10 different measurements on that burst, including time. Second, at the end of each page, (typically 1/2 hour/page) a statistical summary (mean and standard deviation)

# M 7 B COMPUTER PROGRAMS

Figure 1:

(This figure

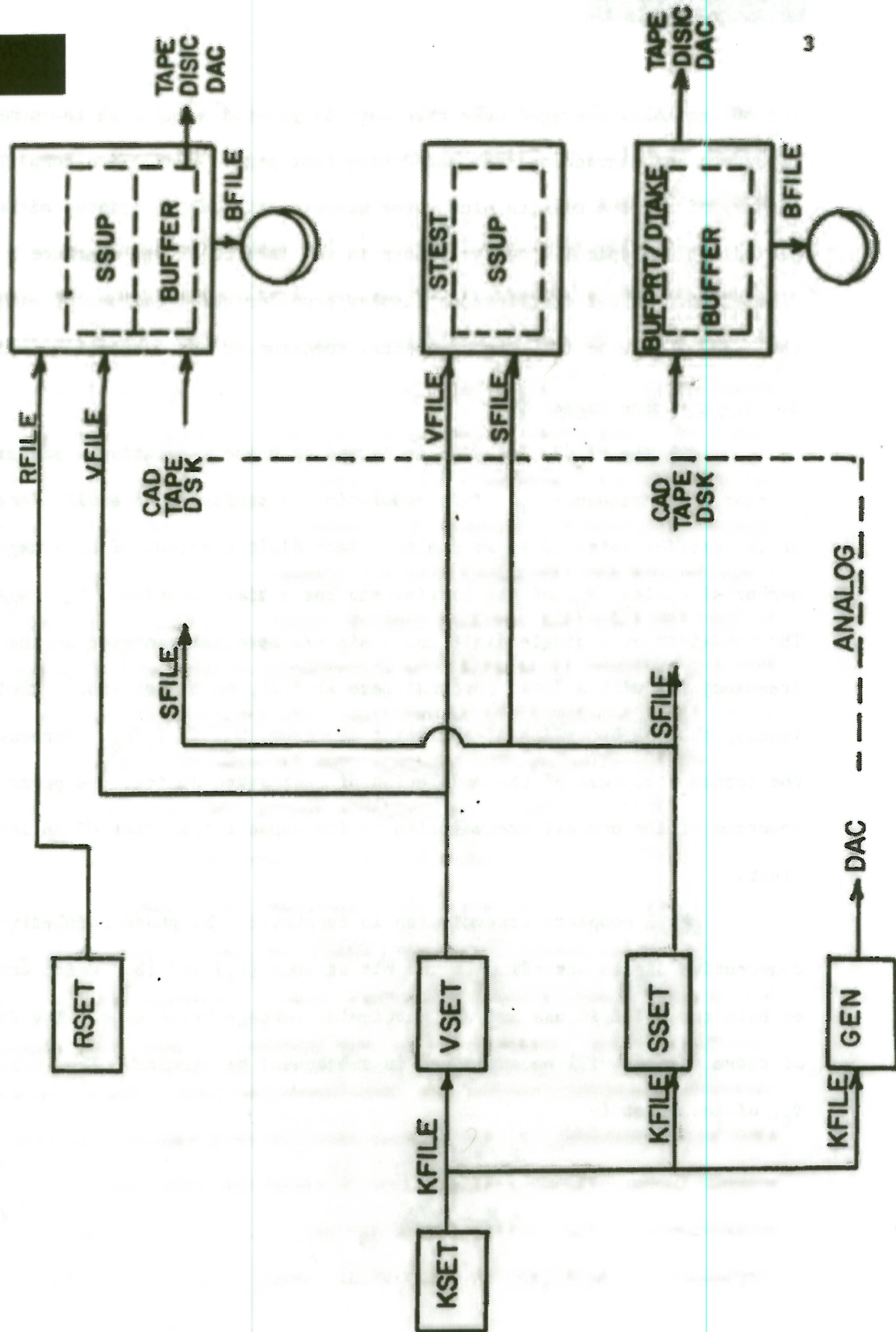


Figure 1: M7B Computer Programs

(This figure



for 50 variables averaged over that page is printed along with the number of bursts and characters received during that page. Finally, a complete summary of all the results plus error measurements can be printed either periodically (typically every 4 hours in the lab) or at the operator's discretion. An X-Y oscilloscope display provides the magnitude of either the channel impulse response or channel spectrum at the operator's choice.

### 3. Transmission Format

The M7 transmission is formed by phase modulating a sinusoidal carrier at a frequency  $f_T$ . This modulation is performed on small pieces of the carrier referred to as digits. Each digit consists of an integer number of cycles,  $N_Q$ , of the carrier and has a time duration,  $T_D = N_Q/f_T$ . The bandwidth of a single digit has a  $\sin x/x$  spectrum centered on the carrier frequency and with a first spectral zero at  $f_T/N_Q$  on either side. Equivalently, the 4dB bandwidth of the digit spectrum,  $W_D$ , is  $f_T/N_Q$ . Because of the random structure of the modulation of successive digits, the power spectrum of the overall transmission is (in expectation) that of an individual digit.

A complete transmission is constructed by phase modulating  $N_B$  consecutive digits according to two bit streams  $\{a_i\}$  and  $\{b_i\}$  which are based on both the KFILE in use and the particular message being sent. The derivation of these streams will be explained in subsequent paragraphs. The total duration,  $T_B$ , of the burst is

$$T_B = N_B \cdot T_D \quad (1)$$

$$= N_B \cdot N_Q / f_T \quad (2)$$

Taking the 4 dB digit bandwidth,  $W_D$ , as the system bandwidth yields the following result for the transmission TW product:

$$T_B \cdot W_D = N_D \cdot N_Q / f_T \quad f_T / N_Q \quad (3)$$

$$= N_B \quad (4)$$

Thus, the transmission TW product equals the number of digits in the burst,  $N_B$ . In current versions of the system,  $N_B$  is constrained to be a power of 2.

$N_A$ -ary biorthogonal signalling is used to impose the information on each burst. Although the name sounds esoteric, the technique is not difficult to understand. The parameter  $N_A$  is the number of different symbols which can be transmitted in a given symbol position. For example, in dialing a telephone  $N_A = 10$  as only the integers 0...9 can be used. In order to facilitate the conversion between bit patterns and symbols,  $N_A$  is required to be a power of 2 in the current system. This means  $N_L$  bits are contained in each symbol, where

$$N_L = \log_2 N_A \quad (5)$$

will always be an integer. The symbols are biorthogonal in signal space in that for any two different symbols, either the symbols are orthogonal to each other or the symbols are the negative of each other. The reason for this choice is beyond the scope of the present paper.

Each burst of  $N_B$  digits is divided into  $N_G$  symbol positions, that is, there are  $N_G$  symbols per burst. To maintain homogeneity among the symbols in error performance, the number of digits in each of the  $N_G$  symbol positions should be nearly constant. Because  $N_G$  may not divide  $N_B$  perfectly, the number of digits per symbol position can't always be made equal for a given



choice of  $N_B$  and  $N_G$ . In the current system, the  $N_B$  digits are divided into  $N_G-1$  symbol positions of  $N_S$  digits each, plus one slightly longer final symbol of  $N_{S(LAST)}$  digits. Because of the structure of the current system,  $N_S$  must also be a multiple of 16. The equations for  $N_S$  and  $N_{S(LAST)}$  are then

$$N_S = \text{INT} \left[ \frac{N_B}{16 \cdot N_G} \right] \cdot 16 \quad (6)$$

$$N_{S(LAST)} = N_B - (N_G-1) \cdot N_S \quad (7)$$

where  $\text{INT}[x]$  is the "integer part of  $x$ " function, i.e.  $\text{INT}[8/3] = 2$ .

If  $N_G$  happens to be a power of 2, then  $N_S = N_{S(LAST)}$  and the symbol positions have the same number of digits. In practical cases considered to date,  $N_S$  and  $N_{S(LAST)}$  differ only slightly (i.e. 5%).

As indicated above, the phase modulation of the  $N_B$  digits is based on two bit streams  $\{a(i)\}$  and  $\{b(i)\}$ . Both streams are derived from the random bit stream,  $\{k(i)\}$  contained in the KFILE. The random bit stream  $\{k(i)\}$  must contain  $N_B \cdot (1 + (N_A/2))$  bits. The stream  $\{a(i)\}$  is called the probe bit stream and is simply the first  $N_B$  bits from  $\{k(i)\}$ :

$$a(i) = k(i) \quad i = 0 \dots N_B-1 \quad (8)$$

where each  $k(i)$  is either zero or one.

The second bit stream,  $\{b(i)\}$ , is called the information stream and is derived from the information being transmitted as well as the bit stream  $\{k(i)\}$ . Let  $\{I(k)\}$  be the information bits to be transmitted where  $I(k)$  is either zero or one. The sequence  $\{I(k)\}$  has  $N_G \cdot N_L$  bit values as there are  $N_G$  symbol positions capable of conveying  $N_L$  bits each. From  $\{I(k)\}$  two  $N_G$  long sequences can be derived which are useful in subsequent work:

$$\text{SYM}(l) = \sum_{r=0}^{N_L-2} 2^{(N_L-2)-r} I(N_L \cdot l + r), \quad l = 0 \dots N_G-1 \quad (9)$$

$$\text{SYMSGN}(l) = I(N_L \cdot l + N_L - 1), \quad l = 0 \dots N_G-1 \quad (10)$$

$\text{SYM}(l)$  is simply the usual integer representation of the first  $N_L-1$  bits of the  $l$ -th symbol position. For example, if  $N_L = 4$ ,  $N_G = 2$  and  $\{I(k)\} = 1, 0, 1, 1, 0, 0, 1, 0$ , then  $\{\text{SYM}(l)\} = 5, 1$ .  $\text{SYMSGN}(l)$  is the  $N_L$ th bit in the  $l$ -th symbol position. In the preceding example,  $\{\text{SYMSGN}(l)\} = 1, 0$ .

The information stream  $\{b(i)\}$  may be derived based on  $\text{SYM}(l)$  and  $\text{SYMSGN}(l)$ . Define  $\tilde{l}$  as follows:

$$\tilde{l}(i) = \text{INT}[i/N_S] \quad 0 \leq i < (N_S \cdot N_G) - 1 \quad (11)$$

$$= N_G \quad \text{otherwise} \quad (12)$$

Thus,  $\tilde{l}(i)$  is the index of the symbol position to which the  $i$ -th digit belongs. The condition in Equations 11 and 12 is necessary because  $N_{S(\text{LAST})} > N_S$ , which could yield  $\tilde{l}(i) > N_G - 1$  if it were not imposed. The information sequence  $\{b(i)\}$  can then be written:

$$b(i) = \text{SYMSGN}(\tilde{l}(i)) \oplus k(N_B + N_S \left[ (N_A/2) \tilde{l}(i) + \text{SYM}(\tilde{l}(i)) \right] + 1) \quad i = 0 \dots N_B - 1 \quad (13)$$

Where  $\oplus$  indicates module 2 addition.

Equation 13 can best be understood in conjunction with Figure 2.

The first  $N_B$  bits of  $\{k(i)\}$  are used to form the probe stream marked 'PROBE' in the figure. The next  $N_{A/2} \cdot N_S$  bits form  $N_{A/2}$  symbol waveforms for the first symbol position, where each symbol uses  $N_S$  bits. These symbols are represented by the rectangles marked 0 through 7 in the left column of the table. For  $\tilde{l}(i) = 0$ ,



**+ INFO**

**NB - 4096**

← NG = 12 SYMBOLS →

**NSLAST**  
**\* 356**

0	—	8	16	24	—	32	40	48	56	64	72	80	88
1	9	+	17	25	33	41	49	57	65	73	81	89	
2	10		18	26	34	42	50	58	66	74	82	90	
3	—	11	19	27	35	43	—	51	59	67	75	83	91
4		12	20	28	36	44	—	52	+	60	68	84	92
5		13	21	29	37	45	53	61	69	77	85	93	
6		14	22	30	38	46	54	62	+	70	78	86	94
7		15	23	31	39	47	55	63	71	79	87	95	+

$$\leftarrow 8 = NA/2 \rightarrow$$

## INFORMATION

7	1	2	3	1	9	7	8	C	A	F	E
-3	-8	+17	-25	-32	-44	-51	+60	+70	+77	-87	+95
PROBE (CONSTANT)											

**Figure 2:**

M7BX2 TRANSMISSION EXAMPLE ( INFO=7123 1978 CAFE)

(This style)

the first symbol position, Equation 13 becomes:

$$b(i) = \text{SYMSGN}(0) \oplus k(N_B + N_S \cdot \text{SYM}(0) + i) \quad (14)$$

$$i = 0 \dots N_S - 1$$

That is,  $b(i)$  is taken from the symbol specified by  $\text{SYM}(0)$ ; then inverted or not inverted according to  $\text{SYMSGN}(0)$ . In the example,  $\text{SYM}(0) = 3$ ,  $\text{SYMSGN}(0) = 1$ , thus the first  $N_S$  bits are the complement of those in the rectangle marked 3. This is indicated by -3 placed in the first symbol position. Other symbol positions are filled by moving  $N_S \cdot N_A / 2 \cdot i(i)$  bits along the  $\{k(i)\}$  stream and performing the same process.

Note that because of the random structure of  $\{k(i)\}$  there is no relation between the probe and any of the rectangles marked 0...95 nor between the rectangles. This is a key point in the denial of signal processing gain to an interceptor who does not have  $\{k(i)\}$  available.

Given the probe and information bit streams  $\{a(i)\}$  and  $\{b(i)\}$  of length  $N_B$ , the transmission can be easily constructed. First, however, these bit streams must be converted to bipolar form, that is have values of either plus one or minus one. Let

$$\tilde{a}(i) = 2a(i) - 1 \quad i = 0 \dots N_B - 1 \quad (15)$$

$$\tilde{b}(i) = 2b(i) - 1 \quad i = 0 \dots N_B - 1 \quad (16)$$

Further, define  $p(t)$  to be a rectangular baseband pulse of duration equal to the digit duration,  $T_D$ . That is

$$p(t) = 1 \quad 0 \leq t < T_D \quad (17)$$

$$= 0 \quad \text{otherwise} \quad (18)$$



Then the M7 transmitter output,  $m(t)$ , is given by

$$m(t) = \sum_{i=0}^{N_B-1} p(t-i T_D) \left\{ \tilde{a}(i) \cos 2\pi f_T t - \tilde{b}(i) \sin 2\pi f_T t \right\} \quad (19)$$

Since  $\tilde{a}(i)$  and  $\tilde{b}(i)$  are bipolar, the  $i$ -th transmitted digit consists of a cosine component, whose sign is set by the probe stream,  $\tilde{a}(i)$ , plus a sine component, whose sign is set by the information stream,  $\tilde{b}(i)$ .

Figure 3 depicts these components, with the resultant vectors labelled  $(\tilde{a}(i), \tilde{b}(i))$ . Note that because of the symmetry of the modulation and the randomness underlying  $\{\tilde{a}(i)\}$ ,  $\{\tilde{b}(i)\}$ , the average of the transmission over the burst will be zero. This means that the spectrum of the burst will have no discernible carrier.

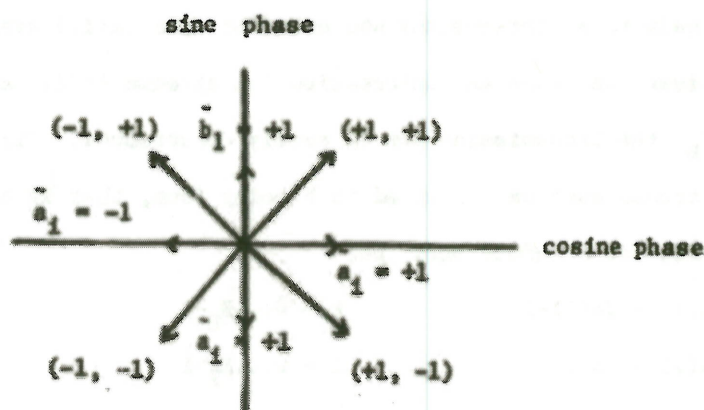


Figure 3: Digit modulation alternatives.  
(This figure

Although the absence of a carrier line in the transmission spectrum is essential for a practical system, it prevents the concurrent processing of the signal by traditional (CW) methods. Since evaluation of the system must be done in cooperation with other (CW) studies, the existing transmitter has been designed to inject a specified amount of carrier if necessary. This allows the transmission to be processed both the M7 system and traditional CW methods without appreciably reducing either's performance. With this modification, Equation 19 becomes:

$$m(t) = \sum_{i=0}^{N_B-1} p(t-iT_D) \{ \bar{a}(i) \cos 2\pi f_T t - \bar{b}(i) \sin 2\pi f_T t \} + K_{CI} \cos 2\pi f_T t \quad (20)$$

where  $K_{CI}$  is the carrier injection coefficient. If  $K_{CI} = 2$ , then equal amounts of signal energy are contained in the burst and in the carrier while the burst is on.



#### 4. Receiver Operation and Results

##### 4.1 General Operation

■ An overview of the M7 receiver operation is presented in this section to enable the reader to understand the many results produced on-line and in real time by the receiver. Operation of the receiver can be considered in terms of two independent processes: synchronization and demodulation. Synchronization is the process by which the presence or absence of an M7 signal is determined; if the signal is present preliminary estimate of its time and frequency location is provided. If a signal is present, the demodulation process is initiated, which removes any residual Doppler from the signal and makes the necessary symbol decisions.

■ During operation, the receiver prints results on both the teleprinter and line printer; producing line summaries, page summaries and block summaries, as well as a printout of the message. The block summary is a single 8-1/2 x 11 sheet summarizing all results over a selected period of time, typically several hours. Although the block summary has the most densely packed results, it is the best one on which to learn to interpret the system outputs. Consequently, the discussion of line summaries, page summaries and message printouts will be deferred until later.

■ Figure 4 depicts a typical block summary, along with hand annotation of relevant outputs. The top-most encircled line identifies the receiver date and the time interval over which the data is summarized. The quantities in parentheses give the duration of the interval in HOUR:MIN format. When using the receiver, the computer program date should be verified to be that of the latest revision. The times are indicated in the format DAY:HOURL:MIN, where DAY is the day of the year.

The second block from the top identifies the particular version of the receiver in use, as specified by the contents of the RFILE. All of the parameters associated with the version are printed. The parameters NA, NB, NC, NL, NQ, NS and  $NSL = N_{S(LAST)}$  were defined in the preceding section, the remaining parameters will be defined later.

The third block from the top defines the VFILE in use. Because of an interlock, the parameters of this VFILE necessarily correspond to those of the RFILE. The first 4 lines in this block are the VFILE identification, which is identical to the KFILE identification. The quantity  $N_K$  is the decimation factor used in generating the sequence  $\{k(i)\}$  in the KFILE, the quantities NIV, NOV are parameters dealing with the construction of the VFILE and will be described later.

The fourth block from the top describes the data being applied to the receiver. If the input is analog, the data header is entered by the operator, if the input is from tape, the data header is taken from the tape. The data header contains the starting time of the data and the receiver center frequency,  $f_R$  and  $N_Q$ . While the value of  $N_Q$  placed in the data header by the operator must agree with that of the RFILE, the center frequency can be adjusted to meet particular operating conditions. Also included in the data header is the frequency of the sampling clock, which is always equal to  $4*f_R$ .

Finally, in the lower right hand corner is a block labeled NDBV( X ) with two numbers below it. This represents the average input level in dB relative to one volt, as measured at periodic intervals. The quantity X is the number of such measurements taken, the first number below it is the mean value, the second below it is the standard deviation. The measurement NDBV



Figure 4: Block Summary: Identifying Labels  
(this figure classified)

14

RECVR : 11 FEB 79A - BLOCK SUMMARY : 50: 8: 33 TO 51: 22: 18 ( 37: 45 )

'BXSA - SPECIAL HIGH RATE VERSION FOR '78 NSUA  
NH0 = 16 , INFO = NSUA-NUSC780

RFILE

30 OCT 78 AT 1109 HR ( RETYPED 05 JAN 78 AT 0757 HR )

NA	NB	ND	NE	NG	NH0	NH1	NI	NL	NM	NO	NO	NS	NSL	NT0	NT1	NW
64	4096	15	2048	10	16	256	512	6	240	32	4	409	415	2	5	16

ZSHLIM	FTHRS0	FTHRS1	R2CUT0	R2CUT1	R2CUT2	DF1	DF2	NE1	INVFL0
0.200	3.235	3.730	0.100	0.100	0.100	1.000	1.000	4036	0

K12013

K STREAM FOR M7BX5

KFILE / VFILE

12 OCT 78 AT 1330 HR

NH : 4 NIV : 512 NOV : 32

M7BX5 THROUGH CELTHRA CHANNEL AT -8.0 DB

TWIST = 119. ( 21.5 KT ) , INFO = NSUA-NUSC78

DATA

15 FEB 79 AT 0833 HR

STARTING TIME : 50 : 8 : 33 : 0

NO = 4

CENTER FREQUENCY : 204.800

CLOCK FREQUENCY : 0 819. 200

583. BURSTS

5830. SYMBOLS

34980. BITS

2.7

2. SYMBOL ERRORS

0.000343/ 0.000343 PE(SYM)

SYMBOL ERRORS BY LOCATION :

1.	0.	0.	0.	0.	0.	0.	1.
0.	0.						
1.	0.	0.	0.	0.	0.	0.	1.
0.	0.						

L0	L1	L2	L3	TS0	TS1	TS2	TS3
5.38	8.13	13.85	26.43	-28.	0.	-0.	1.
1.33	0.76	1.12	1.49	1483.	2.	2.	2.

FS0	FS1	FS2	FS3	F2	F2A	F2B	F3	F3A	F3B
118.64	118.64	118.68	118.96	118.65	118.97	118.97	118.98	118.98	118.98
0.32	0.24	0.08	0.08	0.24	0.05	0.05	0.06	0.08	0.01

R2	R2A	R2B	R3	R3A	R3B	A2	A2A	A2B	A3	A3A	A3B
0.746	0.697	0.762	0.918	0.858	0.885	0.153	0.000	0.001	0.000	0.000	0.001
0.111	0.105	0.075	0.042	0.057	0.046	0.118	0.018	0.009	0.016	0.003	0.008

TP2A	TP2B	TP3A	TP3B	NZ2A	NZ2B	NZ3A	NZ3B	SNR2A	SNR2B	SNR3A	SNR3B
143.	-359.	137.	-368.	5.	4.	4.	4.	-12.2	-12.2	-9.3	-9.2
51.	51.	58.	59.	1.	1.	1.	1.	0.7	0.7	0.5	0.5

INF2A	INF2B	INF3A	INF3B	SS	LON( 1066. )	LIN( 228. )	NDBV( 75. )
13.1	13.0	13.3	13.2	-3.1	2.73	2.28	-3.6
0.7	0.7	0.6	0.7	0.0	0.15	0.15	0.3

SPEED : 21.5 ( 0.02 ) KTS

OFFSET : 1.487294 ( 0.001055 ) HZ

\*\*\*

\*\*\*

is taken independently of whether signal or noise is present and hence may contain portions of both signal and noise. The primary purpose of computing NDBV is to assure that the input of the A/D converter is not overloaded, which occurs roughly at NDBV = + 3 dBV.

The objective of the synchronization procedure is to determine the presence or absence of the M7 signal; if it is present, a preliminary estimate of its time and frequency location must be produced. Each input complex sample  $x(i)$  is assigned an index number and rotated through a disk buffer file called the BFILE (B for 'buffer'). The primary synchronization search is performed on successive  $N_B$ -long vectors  $\bar{X}_0(i)$  separated by  $N_E$  complex samples.

$$\bar{X}_0(i) = [x(i \cdot N_E), \dots, x(i \cdot N_E + N_B - 1)] \quad (21)$$

If  $N_E < N_B$ , as is usually the case, the vectors  $\bar{X}_0(i)$  overlap. When the primary search indicates a signal may be present in  $\bar{X}_0(i)$ , a secondary search is initiated to better resolve the time and frequency location of the signal. If the results of the secondary search confirm that a signal is present, the demodulation procedure described in the next section is initiated; if the secondary search fails, the receiver continues with a primary search of  $\bar{X}_0(i + 1)$ . Figure 5 is helpful in visualizing the synchronization process.

If the receiver enters the information processing procedure, the data is displaced by an additional amount  $N_{E1}$  to make up for the additional time spent in information processing.

$$\bar{X}_0(i + 1) = [x(i \cdot N_E + N_E + N_{E1}) \dots x(i \cdot N_E + N_E + N_{E1} + N_B - 1)]$$

(Post Demodulation)      (22)



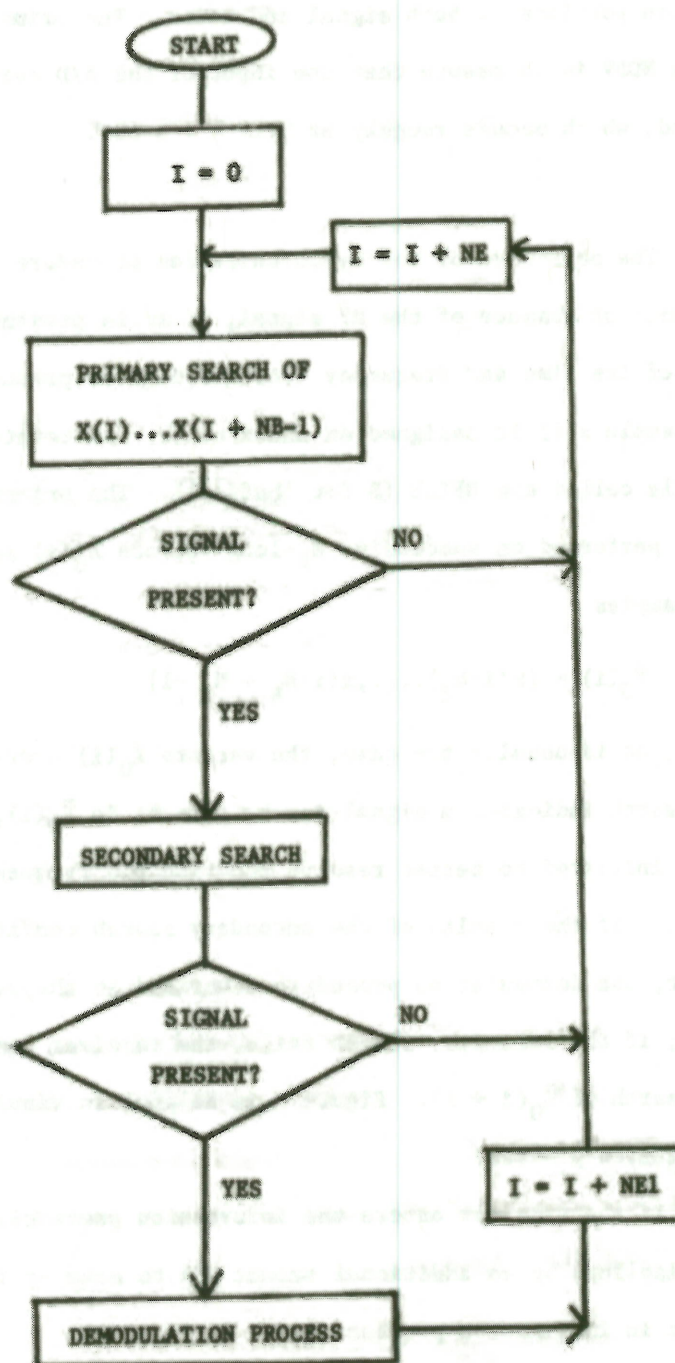


Figure 5. Receiver operation overview. (This figure

This gives rise to a period of receiver blanking of duration  $N_E + N_{E1}$  after every entry (false alarms too!) into the information procedure. Consequently, messages that are sent too close together or which follow a false alarm may be missed. Current values of  $N_E$  and  $N_{E1}$  are sufficient to assure that signals sent at a 50% or less duty factor will not be missed because of receiver blanking unless a false alarm occurs.

#### 4.2 Synchronization

All the details of the primary search will not be presented here, however, meaning of the parameters related to it will be given. The objective of the primary search is to determine whether signal is present within the vector of input samples,  $X_0(i)$ , presented to it. Because the signal may start or end at any point in the vector and may be located at a substantial Doppler offset from the receiver center frequency,  $f_R$ , the primary synchronization task is formidable. The search is performed over several Doppler offsets and effectively all possible time offsets, to obtain the primary search output,  $L\phi$ , and the estimated time and frequency locations of the signal  $TS\phi$  and  $FS\phi$ .

The structure of the frequency search is worth noting. For convenience, frequency offsets are considered in terms of line spacings of the Fourier transform of the  $N_B$  output points rather than in Hertz. This makes interpretation of the frequency offsets independent of frequency and system  $Q$ ,  $N_Q$ . The spacing between spectral lines in Hertz is the reciprocal of the  $N_B$ -long block duration.

$$DFLINE = \frac{f_R}{N_Q N_B} \quad (23)$$



A frequency shift of  $DF_{Hz}$  Hertz is then equal to the following offset in terms of spectral lines:

$$DF = \frac{DF_{Hz}}{DFLINE} \quad (24)$$

Unless explicitly labelled as being in Hertz, the output results of the receiver are in terms of spectral line spacings as indicated by Equation 22 above. Because of the structure of subroutines internal to the receiver, the sign of all frequency offsets is inverted from the usual notion. That is, a signal received at  $DF = +10$  actually is below the receiver frequency  $f_R$ , not above it.

For small amounts of Doppler, Doppler on a wideband signal can be considered as a frequency shift. The Doppler search can then be conducted by simply offsetting the transform of the input by an integer number of spectral lines,  $k$ . In order to increase the detectability of the signal, however, a finer grain search may be called for. The search algorithm in the receiver provides for this by permitting  $N_{T\phi}$  searches within a given line width. Thus, the resolution in Hertz of the search process is

$$DF_{RESOLUTION(Hz)} = \frac{f_R}{N_Q \cdot N_B \cdot N_{T\phi}} \quad (25)$$

Let the total width of the search be  $N_W$  spectral lines ( $\pm NW/2$  lines) or

$$DF_{RANGE(Hz)} = \frac{f_R}{N_Q \cdot N_B} \cdot N_W \quad (26)$$

Thus for small amounts of Doppler,  $N_W$  specifies the Doppler range being searched, whereas  $N_{T\phi}$  indicates the spacing of the search.

For non-trivial amounts of Doppler ( $\sim \pm 8$  spectral lines), the time dilation effects of Doppler must be taken into account or

dramatically reduced performance results. This is handled in the M7 receiver by generating  $N_D$ -time dilated waveforms separated by  $N_W$  spectral lines. A search of  $\pm N_W/2$  spectral lines is performed about each waveform, so that the Doppler offset between the input and the correlator waveform is at most  $N_W/2$  spectral lines. The frequency interval of width  $N_W$  centered on a time dilated correlator waveform is called a time dilation bin. This yields a total search range of  $N_M$  spectral lines where

$$N_M = N_W \cdot N_D \quad (27)$$

The total search range in Hertz is:

$$DF_{RANGE}(Hz) = \frac{f_R}{N_Q \cdot N_B} \cdot N_M \quad (28)$$

For convenience,  $N_D$  is constrained to be odd by the current version of the receiver. This assures that one of the correlator waveforms is un-dilated (i.e., at zero Doppler). Figure 6 is helpful in visualizing the parameters  $N_W$ ,  $N_{T\phi}$ , and  $N_M$ .

At each Doppler offset, the receiver calculates the cross-correlation of the input vector  $\bar{X}(i)$  with the transmitted probe waveform. Since the spectrum of the probe waveform is nearly white because of the randomness of the  $\{a_i\}$  stream, the cross correlator output approximates the impulse response of the channel. The correlator output is squared to provide an energy measurement, and then summed over  $N_{H\phi}$  samples starting at each possible time offset,  $i$ ,  $0 \leq i < N_B$ . Let  $y(i,k)$  be the (complex) correlator output,  $0 \leq i < N_B$  at the  $k$ th Doppler offset. Then the summer output  $z(j,k)$  for a time offset  $j$  and Doppler offset  $k$  is simply:





(This figure [REDACTED])

$$\begin{aligned}
 i &= j + (N_{H\phi} - 1) \\
 z(j, k) &= \sum_{i=j}^{i=j+(N_{H\phi}-1)} |y(i, k)|^2 \\
 i &= j
 \end{aligned}
 \tag{29}$$

where the index is calculated modulo  $N_B$ . Because of the excellent ambiguity function (in expectation) of the transmitted probe waveform,  $z(j, k)$  can be expected to reach a maximum when  $k^*$  is the Doppler offset closest to the received signal. Likewise  $z(j, k^*)$  can be expected to reach a maximum when the index  $j^*$  specifies the start of the most energetic segment of the channel impulse response. The output of the primary synchronization procedure  $l_0$ , is then

$$\begin{aligned}
 l_\phi &= \frac{\frac{1}{N_{H\phi}} \max_k \{ \max_{0 \leq j < N_B} z(j, k) \}}{\frac{1}{N_B} \sum_{i=0}^{N_B-1} |x(i)|^2} \\
 i &= 0
 \end{aligned}
 \tag{30}$$

Here the factor  $1/N_{H\phi}$  and the denominator serve to normalize the output against changes in input level. If the channel is ideal and no noise is present,  $l_0$  takes on the value  $N_B/N_{H\phi}$ . Let  $j^*$ ,  $k^*$  represent the time and Doppler indices for which the maximum is attained.

The final step of the primary synchronization is to compare  $l_0$  with a prescribed threshold,  $FTHR\phi$ . If  $l_0$  is below the threshold, a "signal not present" decision is made and the search is initiated over a later data vector. The synchronization output,  $l_0$ , is saved as the result  $L\phi N$ . If  $l_0$  exceeds the threshold,  $FTHR\phi$ , the secondary search is initiated. Furthermore, the following results are saved:  $L\phi = l_0$ ,  $TS\phi = j^*$ , and  $FS\phi = k^*$ . The indices of the maximum,  $j^*$ ,  $k^*$  are passed to the secondary search.



At first glance, a secondary search does not seem necessary as an estimate of the time and frequency location  $(j^*, k^*)$  are available at the conclusion of the primary search. In fact, a secondary search is necessary for two reasons. First, the primary synchronization output,  $l_0$ , could have been obtained as a result of a signal starting at either  $i_0 + j^*$  or at  $i_0 + j^* - N_B$ , where  $i_0$  is the index of the first complex sample of the vector  $\bar{X}_0(k)$  processed in the primary synchronization. This ambiguity of  $N_B$  complex points must certainly be resolved. Second, better overall performance can be achieved if the search is repeated with the input vector more closely aligned with the input signal and with a finer resolution in the frequency search.

The secondary synchronization search involves the same calculation performed in the primary search, but acts on different vectors and with a different Doppler search range. Two input vectors are searched, one beginning ahead of  $\bar{X}_0(1)$ ,  $\bar{X}_1^-(1)$  and one behind  $\bar{X}_0(1)$ ,  $\bar{X}_1^+(1)$ .

$$\bar{X}_1^-(1) = [ x(i \cdot N_E + j^* - N_B), \dots, x(i \cdot N_E + j^* - 1) ] \quad (31)$$

$$\bar{X}_1^+(1) = [ x(i \cdot N_E + j^*), \dots, x(i \cdot N_E + j^* + N_B - 1) ] \quad (32)$$

In order to save computation time, the search is limited to a range of  $\pm DF1$  spectral lines centered on the estimated Doppler offset  $k^*$ . To provide better frequency resolution, the number of interline searches is taken as  $N_{T1}$  instead of  $N_{T\phi}$  as in the primary search. This yields two secondary synchronization outputs  $l_1^-$ , corresponding to the older data and  $l_1^+$ , corresponding to the more recent data. With each of these outputs are estimates of the time and frequency locations of the signal,  $j_1^-, j_1^+, k_1^-, k_1^+$ .

The secondary synchronization outputs  $l_1^+, l_1^-$  are compared against the secondary threshold,  $FTHRS1$ . If both outputs are below  $FTHRS1$ , then the statistic  $L1N$  is updated by each value. If one of the values exceeds  $FTHRS1$ ,

say  $\ell_1^{\pm}$ , then information procedure is initiated, and a "signal present" indication is made. The following statistics are set:  $L1 = \ell_1^{\pm}$ ,  $TS1 = \frac{\pm}{J_1}$ ,  $FS1 = k_1^{\pm}$ . The instance where both outputs exceed the threshold is extremely unlikely. The current program processes the earliest segment and then skips over the second.

To facilitate evaluation of the synchronization performance, bursts are usually transmitted at a specified duty cycle so that the number of complex samples between successive bursts is known. The receiver calculates the difference in complex samples between detection and designates it as the result DT. For bursts sent at a 50% duty cycle and zero Doppler the difference DT should be simply  $2N_B$ . If DT is found to be  $4N_B$ , a burst has been missed and synchronization performance can be scored appropriately.

Figure 7 depicts the same block summary sheet as in Figure 4, but with parameters and results pertaining to synchronization annotated. In the RFILE header, the parameters related to synchronization are underlined. The first encircled line gives the number of bursts detected, that is the number of times,  $N_{BURST}$ , the information procedure was initiated. Also given are the total number of symbols ( $N_G \cdot N_{BURST}$ ) and bits ( $N_G \cdot N_L \cdot N_{BURST}$ ) contained in these bursts. The variables labelled  $L\phi$ ,  $L1$  are the primary and secondary synchronization outputs given that the thresholds were exceeded. The numbers directly below the labels are the means, the numbers below the means are the standard deviations. The time and frequency estimates for the primary and secondary searches ( $TS\phi$ ,  $TS1$ ,  $FS\phi$ ,  $FS1$ ) are also given. Finally,  $L\phi N(NN)$  and  $L1 N(NN)$  give the primary and secondary synchronization outputs given that the thresholds were not exceeded. The numbers in parentheses indicate the number of points on which the means and standard deviations are based.



Figure 7: Block Summary: Synchronization Outputs  
(This figure classified [REDACTED])

24

RECVR : 11 FEB 79A - BLOCK SUMMARY : 50: 8: 33 TO 51: 22: 18 ( 37: 45)

EXSA - SPECIAL HIGH RATE VERSION FOR '78 NSUA  
NH0 = 16 , INFO = NSUA-NUSC780

30 OCT 78 AT 1105 HR ( RETYPED 05 JAN 78 AT 0757 HR )

NA	NE	ND	NE	NG	NH0	NH1	NI	NL	NH	NO	NO	NS	NSL	NT0	NT1	NW
54	4096	15	2048	10	16	256	512	6	240	32	4	409	415	2	5	16

DSHLIM	FTHRS0	FTHRS1	RZCUT0	RZCUT1	RZCUT2	DF1	DF2	NE1	INVFLG
0.200	3.235	3.730	0.100	0.100	0.100	1.000	1.000	4096	0

412012

K STREAM FOR M7BXS

12 OCT 78 AT 1330 HR

NA : 4 NIV : 512 NOV : 32

M7BXS THROUGH CELTHRA CHANNEL AT -8.0 DB

TWIST = 119. ( 21.5 KT ) , INFO = NSUA-NUSC78

19 FEB 79 AT 0833 HR

STARTING TIME : 50 : 8 : 33 : 0

NO = 4

CENTER FREQUENCY : 204.800

CLOCK FREQUENCY : 9 819. 200

583. BURSTS

5830. SYMBOLS

34980. BITS

2.7 2. SYMBOL ERRORS

0.000343/ 0.000343 PE(SYM)

SYMBOL ERRORS BY LOCATION :

1.	0.	0.	0.	0.	0.	0.	1.
0.	0.	0.	0.	0.	0.	0.	1.
1.	0.	0.	0.	0.	0.	0.	1.
0.	0.	0.	0.	0.	0.	0.	1.

L0	L1
8.38	8.13
1.33	0.78

L2	L3
13.85	26.43
1.12	1.49

TS0	TS1
-28.	0
1483.	2.

TS2	TS3
-0.	1.
2.	2.

F50	F51
118.14	118.64
0.32	0.24

F52	F53
118.98	118.96
0.08	0.08

F2	F2A	F2B	F3	F3A	F3B
118.65	118.97	118.97	118.98	118.98	118.99
0.24	0.05	0.05	0.06	0.08	0.01

R2	R2A	R2B	R3	R3A	R3B
0.741	0.687	0.762	0.818	0.858	0.889
0.111	0.105	0.075	0.042	0.057	0.046

A2	A2A	A2B	A3	A3A	A3B
0.152	0.000	0.001	0.000	0.000	0.001
0.118	0.018	0.009	0.016	0.003	0.008

TP2A	TP2B	TP3A	TP3B
143.	-359.	137.	-366.
61.	61.	58.	59.

NZ2A	NZ2B	NZ3A	NZ3B	SNR2A	SNR2B	SNR3A	SNR3B
5.	4.	4.	4.	-12.2	-12.2	-9.2	-9.2
1.	1.	1.	1.	0.7	0.7	0.5	0.5

INF2A	INF2B	INF3A	INF3B
13.1	13.0	13.3	13.2
0.7	0.7	0.6	0.7

S3
-3.1
0.0

LIN( 1088. )	LIN( 228. )
2.73	2.26
0.15	0.15

NDBV( 75. )
-3.8
0.3

FEEL : 21.5 ( 0.02 ) KTS

OFFSET : 1.487294 ( 0.001059 ) HZ

\*\*\*

\*\*\*

### 4.3 Demodulation

At the conclusion of the synchronization process, the demodulation process is initiated if a "signal present" decision was made. Estimates of the signal's time and Doppler location are available when demodulation begins. The demodulation process consists of 2 steps: an initial demodulation to determine the symbols transmitted followed by a bootstrap demodulation based on a higher quality channel measurement. Figure 8 provides a flow chart for the overall demodulation process. Note that each demodulation step consists of 5 operations: frequency shifting, a search, further frequency shifting, channel impulse response measurement and symbol decision making.

#### 4.3.1 Initial demodulation

The first step in either the initial or final demodulation is to shift the signal to zero frequency via the ZSHIFT algorithm. This algorithm is applied to the data six times throughout the demodulation process. The ZSHIFT algorithm takes the time dilation effects of Doppler into account. This is done by interpolating the data at a rate corresponding to the Doppler offset found during synchronization. In the current program, a  $\text{sinc}/x$  interpolation function is used with  $N_0$ -th order interpolation. Because the calculation of the requisite  $\text{sinc}/x$  function is time consuming for the  $N_B \cdot N_0$  points required for the interpolation, the  $\text{sinc}/x$  function is calculated from tabular values. In the current program, the table values have  $N_I$  points between zeros. Since the function is symmetric, only  $N_0 \cdot N_{I/2}$  points of  $\text{sinc}/x$  need be computed, a considerable savings in time. The use of tabular values for  $\text{sinc}/x$  results in a trivial increase in interpolation error.



Figure 8: Demodulation Flow Chart

(This figure classified [REDACTED])

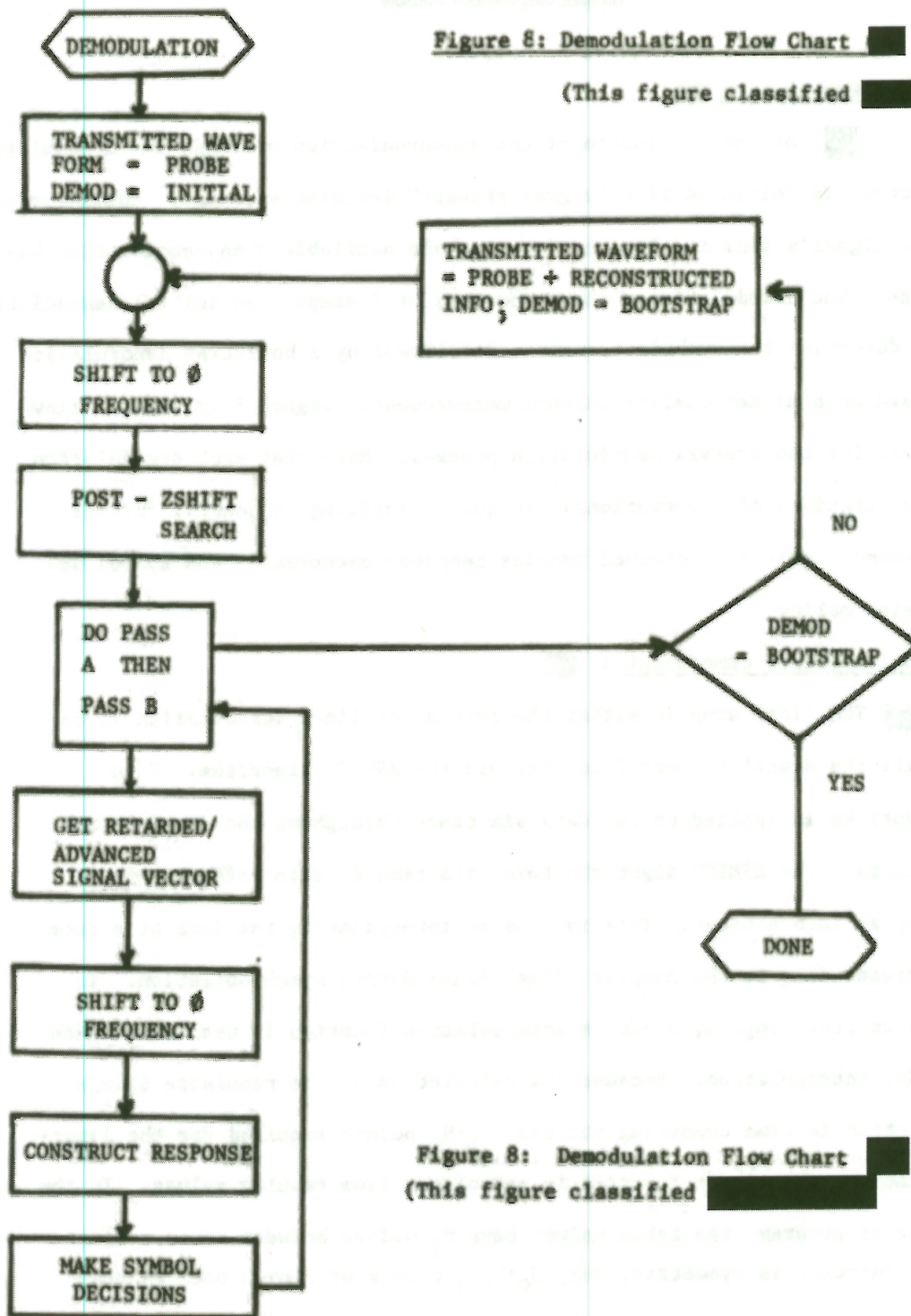


Figure 8: Demodulation Flow Chart

(This figure classified [REDACTED])

Before continuing the description of the shift to zero Doppler, note that the variables NIV, NOV in the VFILE header have the same roles as  $N_I$ ,  $N_O$  in the construction of the VFILE. They are used to construct the  $N_D$  time-dilated representations of the probe component, as required by the synchronization procedure. Although  $N_{IV}$ ,  $N_I$  and  $N_{OV}$ ,  $N_O$  are equal in current versions, no interlock is enforced. Thus the quality of interpolation for the synchronization vectors can be different from that in the demodulation process.

The shift to zero Doppler is not complete after the above mentioned interpolation, as some slight residual phase shift across the input vector might remain. Since the sign of filter outputs is important in determining the symbol values, such a phase shift must be minimized. This is accomplished by partitioning the signal into two halves and construction the channel impulse response from each half. To improve the quality of these responses, they are filtered in the time domain by a procedure described under the channel measurement operation below. Two parameters involved in this filtering are  $N_{H1}$ , the width of the time window and R2CUT0, the threshold on magnitude squared. The complex correlation between the two halves is then calculated and the angle of the correlation yields the final frequency shift required to achieve zero Doppler. To preclude excessive final frequency shifts at low S/N, the magnitude of the final frequency shift is constrained to be less than the parameter ZSHLIM.



■ The results of the shift to zero Doppler is expressed in the measurement of the frequency of the incoming transmission, designated F2. At the conclusion of the shift, the complex correlation coefficient is recomputed, to give an indication of any residual Doppler. This yields two additional measurements: R2 which is the magnitude of the normalized correlation coefficient and A2 which is the angle, in revolutions ( $360^\circ = 1$ ), of the coefficient.

■ Each application of the ZSHIFT algorithm yields three variables: the frequency measured FN, the magnitude of the correlation coefficient, RN, and the angle of the correlation coefficient AN.

■ The second step in either demodulation process is to re-apply the SEARCH algorithm to the signal which is presumably at zero frequency. This seemingly needless function is in fact important because the frequency estimate from the earlier search is subject to distortion due to time dilation effects. The ZSHIFT routine brings the signal close enough to zero frequency that the frequency estimate from this search, designated the post-ZSHIFT search, is of high quality. The results of the post-ZSHIFT search are given in the statistical outputs L2, TS2 and FS2, which are the output level, time estimate and frequency estimate, respectively.

■ When a burst of  $N_B$  complex samples is transmitted through the ocean, multipath increases the duration of the received signal beyond  $N_B$  samples. The time location found by the synchronization process effectively locates the start of the most energetic  $N_B$ -long interval containing the signal. In so doing, a portion of either the first symbol

or last symbol may fall outside the interval specified by the synchronization process, which will lead to errors on these symbols. To counter this problem, the receiver processes the signal in two passes: In the first pass, designated the A pass, it acts on a signal retarded by  $N_{H1}$  complex points to determine the first  $N_{G/2}$  symbols. This retarded signal certainly contains all of the first symbol energy, but may miss much of the last symbol. In the second pass, designated the B pass, it acts on a signal advanced by  $N_{H1}$  complex points to determine the last  $N_{G/2}$  symbols. This advanced signal certainly contains all of the last symbol energy but may miss much of the first symbol. Because  $N_{H1}$  is small relative to  $N_B$ , the offsetting process does not significantly effect the subsequent processing of the probe component.

First, the input to the pass is shifted to zero Doppler via the ZSHIFT algorithm. This yields the statistical outputs F2A, F2B, R2A, R2B and A2A, A2B. Because the frequency estimate provided to the ZSHIFT algorithm has been improved by the post-ZSHIFT search, the frequency estimates F2A, F2B are generally better than the earlier estimate F2.

The next operation is to measure the channel impulse response for construction of the symbol matched filters. This is accomplished by crosscorrelating the transmitted probe waveform with the input signal (now at zero Doppler). Two filtering operations in the time domain are applied to the measured response to improve the quality of the estimate.



First, the most energetic contiguous segment of  $N_{H1}$  points is located and all points outside that segment are zeroed. Second, the maximum value of magnitude squared for points within the segment is computed and points within the segment below  $R2CUT1$  times the maximum in magnitude squared are zeroed. This leaves a response with only significant points non zero.

Several important statistics are computed while deriving the channel impulse response estimate. Prior to the filtering operations, the ratio of the energy in the selected  $N_{H1}$ -long interval to that in an interval  $N_B/2$  points away is computed. This forms the basis for the calculation of the estimates of input signal to noise ratio,  $SNR2A$ ,  $SNR2B$ , in dB. Because of the equation employed, these estimates are 3 dB below the actual S/N. Further, the equation employed is applicable only for S/N's below -3 dB. The starting index of the  $N_{H1}$  long interval is saved statistically as  $TP2A$  and  $TP2B$ . Also the number of non-zero points in the channel impulse response is saved as  $NZ2A$  and  $NZ2B$ . The latter quantities provide a good measure of the severity of multipath.

The third operation in the initial demodulation is to make the decisions on the received symbols. This is done by applying matched filters corresponding to each possible symbol. The channel impulse response measurement is used to construct each filter, so that the filters are matched to the received symbol waveform. Because of the way the filters are constructed the correct sampling instant for each filter decision is known. Consequently, there are  $N_G \cdot N_A/2$  signed real numbers corresponding to the outputs of the symbol filters. Symbol decisions are made by choosing the filter output having the largest magnitude (out of  $N_A/2$  filter outputs) for each of the  $N_G$  symbol positions. The sign of the filter output along with the identity of

that filter sets the symbol value.

For non-binary signalling ( $N_A > 2$ ), an interesting statistic based on the symbol filter outputs is computed. Suppose  $N_A = 16$ , then there are 8 filter outputs, 1 which is the maximum which corresponds to the correct symbol and 7 that correspond to the other, presumably incorrect symbols. The ratio in dB of the maximum filter output to the average non-maximum symbol output is calculated for each of  $N_G$  symbol positions. This result is then averaged over  $N_G$  symbol positions and saved as the statistics INF2A, INF2B, providing a good measure of the quality of the symbol decisions. When  $N_A = 2$  (binary signalling) this statistic cannot be computed as there is only one filter output, and INF2A, INF2B are set to zero.

When an RFILE is generated a correct message is specified to be used in evaluating the system error performance. After each demodulation the symbol decisions are scored against this message. A count of errors by symbol position is maintained to aid in locating anomalies in the processing. A total error count is also maintained and an overall probability of a character error PE(CHAR) is computed. The correct message contained in the RFILE effects only the receiver scoring, arbitrary messages are processed and printed without prejudice.

Figure 9 depicts a block summary with the variables in the RFILE header pertaining to initial demodulation underlined and with results from the initial demodulation circled. The meaning of the parameters  $N_{H1}$ ,  $N_I$ ,  $N_O$ , ZSHLIM, R2CUT0 and R2CUT1 has been given above. The circled results have also been explained above. Note, however, the adjacent results of similar annotation appear on the summary. They arise from the bootstrap



Figure 9: Block Summary: Initial Demodulation Outputs

32

(This figure classified [REDACTED])

RECVR : 11 FEB 79A - BLOCK SUMMARY : 50: 8: 33 TO 51: 22: 18 ( 37: 45)

EX3A - SPECIAL HIGH RATE VERSION FOR '78 NSUA  
 NH0 = 16 , INFO = NSUA-NUSC780

30 OCT 78 AT 1105 HR ( RETYPED 05 JAN 78 AT 0757 HR )

NA	NB	ND	NE	NG	NH0	NH1	NI	NL	NM	NO	NC	NS	NSL	NT0	NT1	NW
64	4056	15	2046	10	16	256	512	6	240	32	4	405	415	2	5	16

ZSHLIM	FTHR50	FTHR51	RZCUT0	RZCUT1	RZCUT2	DF1	DF2	NE1	INVFLG
0.200	3.235	3.730	0.100	0.100	0.100	1.000	1.000	4056	0

V12013

K STREAM FOR M7BX5

12 OCT 78 AT 1330 HR

NK : 4 NIV : 512 NOV : 32

M7BX3 THROUGH CELTHRA CHANNEL AT -8.0 DB

TWIST = 115. ( 31.5 KT ) , INFO = NSUA-NUSC78

15 FEB 79 AT 0823 HR

STARTING TIME : 50 : 8 : 33 : 0

NO = 4

CENTER FREQUENCY : 204.800

CLOCK FREQUENCY : 0 819. 200

583. BURSTS

5830. SYMBOLS

34980. BITS

2.7

2. SYMBOL ERRORS

0.000343

0.000343 PER(SYM)

SYMBOL ERRORS BY LOCATION :

1.	0.	0.	0.	0.	0.	0.	1.
1.	0.	0.	0.	0.	0.	0.	1.
0.	0.	0.	0.	0.	0.	0.	1.

L0

8.38

1.33

L1

8.13

0.75

L2

13.85

1.12

L3

26.43

1.49

TS0

-28.

1483.

TS1

0.

2.

TS2

-0.

2.

TS3

1.

2.

FS0

118.84

0.32

FS1

118.64

0.24

FS2

118.98

0.08

FS3

118.98

0.08

F2

118.65

0.24

F2A

118.97

0.05

F2B

118.97

0.05

F3

118.98

0.06

F3A

118.98

0.08

F3E

118.99

0.01

R2

0.745

0.111

R2A

0.897

0.105

R2B

0.762

0.075

R3

0.918

0.042

R3A

0.855

0.057

R3B

0.885

0.046

A2

0.153

0.116

A2A

0.009

0.018

A2B

0.001

0.005

A3

0.000

0.016

A3A

0.000

0.003

A3B

0.001

0.008

TF2A

143.

62.

TF2B

-359.

61.

TF3A

137.

56.

TF3B

-366.

59.

NZ2A

5.

1.

NZ2B

4.

1.

NZ3A

4.

1.

NZ3B

4.

1.

SNR2A

-12.2

0.7

SNR2B

-12.2

0.7

SNR3A

-9.3

0.5

SNR3B

-9.2

0.5

INF2A

13.1

0.7

INF2B

13.0

0.7

INF3A

13.2

0.6

INF3B

13.3

0.7

S2

-3.1

0.0

L0N

1068.)

2.73

L1N

228.)

0.15

L2N

2.28

0.15

L3N

-3.8

0.3

NDEV

( 75.)

SPEED : 21.5 ( 0.02 ) KTS

OFFSET : 1.487294 ( 0.001053 ) HZ

\*\*\*

\*\*\*

[REDACTED]

demodulation described later. Thus, only the first of the error results and those statistical results with a 2 in their label arise from the initial demodulations.

#### 4.3.2 Bootstrap Demodulation [REDACTED]

[REDACTED] The error performance of the M7 system depends on the quality of the channel impulse response measurement. A better response measurement will yield better error performance. Only one half of the transmitted energy (the probe) is known exactly to the receiver and can be used in the response measurement during the initial demodulation. After the initial demodulation, however, the symbol decisions obtained in initial demodulation can be used to form an estimate of the total transmitted signal. If the symbol decisions are correct, this would increase by 3 dB the known part of the received signal, and a better response measurement would result. Bootstrapping is the process by which the decisions made in the initial demodulation are used to improve the quality of the information demodulation.

[REDACTED] In order for bootstrapping to be successful, the preliminary symbol decisions should be very nearly correct. Since the receiver is designed to operate with an initial probability of symbol error of .001, few symbol errors are expected in any single burst. Although no theoretical work on bootstrapping has yet been performed, empirical results indicate that it reduces the symbol error rate under normal operating conditions. Consequently, it has been included in the receiver. The difference in error performance and other parameters between initial and bootstrap operations indicates the sensitivity of these parameters to a 3 dB improvement in probe energy.

[REDACTED]



[REDACTED]

The bootstrap process reconstructs the transmitted waveform based on the symbol decisions from the initial demodulation. This reconstructed waveform is then used in subsequent applications of the zero shifting (ZSHIFT), search (SEARCH) and probe reconstruction (PROBE) algorithms. The order of application of these algorithms is exactly the same as for the initial demodulation. The resulting outputs are completely analogous to those of the initial demodulation, except they contain a 3 in their designation instead of a 2. The only exception occurs in SNR3A, SNR3B which measure the input S/N without the 3 dB offset of SNR2A, SNR2B.

To allow additional flexibility in the bootstrap process, different parameters for the search width DF2 (in place of DF1) and for the probe threshold R2CUT2 (in place of R2CUT1) may be specified. Current versions of the program do not make use of their capability and set the values the same for the initial and bootstrap processes.

Figure 10 depicts the block summary with the RFILE parameters dealing with bootstrapping underlined and with the bootstrap results circled. S3 is simply the energy in the input waveform prior to the bootstrap demodulation. The statistics L3, TS3, FS3, arise from the bootstrap search, the statistics F3, R3, A3 arise from the bootstrap zero shifting process, etc. At the bottom of the page, the frequency offset F3 is converted into both knots and Hertz for convenience. The quantities in parentheses are the standard deviations of the offsets in knots and Hertz. Note that the character error count, character error probability and character errors by location are given in the right most or lower position for the bootstrapping demodulation.

[REDACTED]

Figure 10: Block Summary: Bootstrap Demodulation  
(This figure classified [REDACTED])

35

RECV: 11 FEB 78A - BLOCK SUMMARY: 50: 8: 33 TO 51: 22: 18 ( 37: 45)

78X3A - SPECIAL HIGH RATE VERSION FOR 78 NSUA  
NH0 = 16 , INFO = NSUA-NUSC780

30 OCT 78 AT 1109 HR ( RETYPED 05 JAN 78 AT 0757 HR )

NA	NE	ND	NE	NG	NH0	NH1	NI	NL	NM	NO	NO	NS	NSL	NT0	NT1	NW
64	4096	15	2048	10	16	256	512	6	240	32	4	4096	415	2	5	16

ZSHLIM	FTHRS0	FTHRS1	R2CUT0	R2CUT1	R2CUT2	DF1	DF2	NE1	INVFLG
4.200	3.235	3.730	0.100	0.100	0.100	1.000	1.000	4096	0

K12013

K STREAM FOR M7EX5

12 OCT 78 AT 1330 HR

NK: 4 NIV: 512 NOV: 32

M7EX5 THROUGH CELTHRA CHANNEL AT -2.0 DB

WIND = 119. ( 21.5 KT ) , INFO = NSUA-NUSC78

15 FEB 78 AT 0633 HF

STARTING TIME: 50: 8: 33: 0

NO = 4

CENTER FREQUENCY: 204.800

CLOCK FREQUENCY: 9 819.200

513. BURSTS

5630. SYMBOLS

34980. BITS

2.

2. SYMBOL ERRORS

0.000343/

0.000343 PE(SYM)

SYMBOL ERRORS BY LOCATION:

1.	0.	0.	0.	0.	0.	0.	1.
0.	0.	0.	0.	0.	0.	0.	1.
0.	0.	0.	0.	0.	0.	0.	1.

L0	L1	L2	L3	TS0	TS1	TS2	TS3
8.38	6.13	13.85	26.43	-28.	0.	-0.	1.
1.33	0.78	1.12	1.49	1483.	2.	2.	2.

F00	F01	F02	F03	F2	F2A	F2B	F3	F3A	F3B
118.64	116.64	116.88	116.98	118.65	118.97	118.97	118.98	118.98	118.98
0.32	0.24	0.08	0.02	0.24	0.05	0.05	0.02	0.02	0.01

R2	R2A	R2B	R3	R3A	R3B	A2	A2A	A2B	A3	A3A	A3B
0.745	0.697	0.762	0.916	0.898	0.689	0.153	0.000	0.001	0.000	0.000	0.001
0.111	0.105	0.075	0.042	0.057	0.040	0.118	0.018	0.009	0.016	0.003	0.008

TP2A	TP2B	TP3A	TP3B	NZ2A	NZ2B	NZ3A	NZ3B	SNR2A	SNR2B	SNR3A	SNR3B
143.	-359.	137.	-368.	5.	4.	4.	4.	-12.2	-12.2	-9.3	-9.2
62.	11.	55.	55.	1.	1.	1.	1.	0.7	0.7	0.5	0.5

INP2A	INP2B	INP3A	INP3B	ES	LIN( 1065.)	LIN( 228.)	NDBV( 75.)
13.1	13.0	13.3	13.3	-3.1	2.72	2.28	-3.8
0.7	0.7	0.6	0.7	0.0	0.15	0.15	0.3

SPEED: 21.5 0.033 KTS

OFFSET: 1.467294 0.001059 HZ

\*\*\*

\*\*\*



■ The bootstrap demodulation does have one option not previously described as part of the initial demodulation. In the initial modulation, the received signal is cross-correlated with the transmitted probe waveform. In the spectral domain, this corresponds to the multiplication of the conjugate of the probe spectrum,  $\hat{A}(w)$  times the received signal spectrum  $X(w)$ . Let  $X(w)$  be defined as

$$X(w) = A(w)C(w) + N(w) \quad (33)$$

where  $C(w)$  is the channel spectrum  $N(w)$  is the noise spectrum. Thus, the correlator output  $Y(w)$  is

$$Y(w) = |A(w)|^2 C(w) + A^*(w)N(w) \quad (34)$$

of which the first term is the signal contribution. For the random probe sequences considered  $|A(w)|^2$  is a constant in expectation, but in any particular instance has some ripple. Consequently  $Y(w)$  does not equal  $C(w)$  even in the absence of the noise term.

■ As a low cost feature, the current receiver includes the option of using the inverse filter  $1/A(w)$  rather than the conjugate filter  $A^*(w)$  in deriving the channel impulse measurement. This feature is in effect only if INVFLG in the RFILE header is 1, and then only for the bootstrap demodulation. With inverse filtering  $Y(w)$  becomes

$$\begin{aligned} Y(w) &= \frac{1}{A(w)} [A(w)C(w) + N(w)] \\ &= C(w) + N(w)/A(w) \end{aligned} \quad (35)$$

so that  $Y(w)$  is exactly the channel impulse response in the absence of noise. This feature has been used very little and is not considered likely to improve system error performance.